Advances in Environmental Technology 12(3) 2026, 308-326.

Iranian Reasearch Organization for Science and Technology (IROST)

Advances in Environmental Technology

Journal home page: https://aet.irost.ir

Adsorption of hexavalent chromium from aqueous solution using glucose-derived spherical activated carbon: The role of functional groups

Nguyen Duy Dat[a]*, Quang Sang Huynh[a], My Linh Nguyen[a], Hai Nguyen Tran[b]

[a] *Faculty of Chemical and Food Technology, Ho Chi Minh City University of Technology and Engineering, Viet Nam.*

[b] *Center for Energy and Environmental Materials, Institute of Fundamental and Applied Sciences, Duy Tan University, Da Nang City, Viet Nam.*

ARTICLEINFO

Document Type:
Research Paper

Article history:
Received 23 September 2025
Received in revised form
24 April 2026
Accepted 26 April 2026

Keywords:
Carbon sphere
Hydrothermal carbonization
Hexavalent chromium reduction
Surface functionalization
Water treatment

ABSTRACT

Four glucose-derived spherical carbon materials were developed for Cr(VI) removal from water. The materials were synthesized via: (1) hydrothermal carbonization at 190°C, (2) chemical impregnation with H_2O_2, citric acid (CA), or acrylic acid (AA), and (3) pyrolysis at 900°C to produce activated carbons (AC-H_2O_2, AC-CA, or AC-AA, with AC as the control). Boehm titration and FTIR confirmed the presence of increased oxygen-containing groups (carboxyl, lactone, phenol) post-activation. The pH_{PZC} followed the order: 7.10 (AC) > 6.98 (AC-H_2O_2) > 5.89 (AC-AA) > 5.58 (AC-CA). Adsorption was pH (2.0–10) and ionic strength (0–1 M NaCl) dependent, with optimal conditions at pH 2.0 and 0 M NaCl. Kinetics reached equilibrium within 180–360 min, fitting the Elovich model. Equilibrium data were better fit by the Redlich–Peterson and Langmuir models than by the Freundlich model. Langmuir maximum capacities for total Cr were 243.9 mg/g (AC-AA), 240.1 mg/g (AC-H2O), 239.7 mg/g (AC-CA), and 165.3 mg/g (AC). Capacity decreased across water matrices: distilled > drinking > tap > groundwater > lake > river water. Thermodynamics revealed an endothermic ($\Delta H°$>0) and physical adsorption process ($\Delta H°$= 2.34–5.37 kJ/mol). Total Cr recovery was ~70% (0.05 M NaOH), ~20% (0.05 M HCl), and ~10% (hot water at 60°C). Post-adsorption speciation at pH 2.0–4.0 revealed that while Cr(VI) remained the dominant species, a small fraction of Cr(III) was detected in the solution, confirming the partial reduction of Cr(VI). Mechanisms involved electrostatic interactions, surface complexation, and Cr(VI)-to-Cr(III) reduction facilitated by oxygen-containing groups. These functionalized glucose-based spheres offer a sustainable, cost-effective solution for Cr(VI) remediation.

*Corresponding author Tel.: +84 903 056285
E-mail: datnd@hcmute.edu.vn
DOI: 10.22104/aet.2026.7860.2207

1. Introduction

A wide range of human activities, such as industrial processes, agricultural practices, and transportation, release heavy metals that can directly contaminate water sources or disperse into the atmosphere, settle as dust, and eventually be carried into waterways, resulting in substantial water pollution [1, 2]. For example, the application of pesticides, particularly phosphorus fertilizers, can result in the discharge of toxic metals, such as arsenic (As), lead (Pb), and mercury (Hg), into water bodies [3]. The presence of heavy metals in aqueous effluents is a significant concern due to their toxicity and carcinogenic effects on aquatic life and human health [4]. Heavy metals have long-lasting characteristics in the environment, resulting in a range of health problems: dissolve in water, build up in plants and animals, and enter the human food chain via polluted water or food [5]. The unregulated release of heavy metals into the environment poses substantial hazards due to their toxic effects on living organisms [6].

Among these metals, chromium stands out as particularly toxic, occurring in two prevalent forms: hexavalent chromium Cr(VI) is more toxic than trivalent chromium Cr(III), causing severe health issues, including cancer, respiratory problems, and skin ulcers [7, 8]. According to the World Health Organisation, hexavalent chromium is classified as a carcinogen and is among the 50 most dangerous compounds worldwide [9, 10]. It is commonly detected in soil and groundwater at industrial sites due to its use in dyes, paints, and tannery wastewater [11]. While the volume of wastewater generated by electroplating and metal plating companies may not be as substantial as that of other sectors, such as the paper or textile industries, it does contain significant amounts of hazardous substances, notably chromium [12].

The study of heavy metal removal from water via adsorption has been extensively explored worldwide. A previous study investigated the use of agricultural by-products, such as bagasse, banana peels, coconut fibre, sawdust, corn husks, rice husks, straw, and peanut shells, for the adsorptive removal of heavy metals from water, with these materials modified with phosphoric acid [13]. Similarly, the previous study prepared biochar from Tectona grandis sawdust, activating it with K_2CO_3 and $ZnCl_2$, which achieved a surprisingly high Cr(VI) maximum adsorption capacity ranging from 103 mg/g to 127 mg/g [14]. A maximum chromium adsorption capacity of 176 mg/g was obtained using KOH-modified activated carbon derived from corn straw [15]. Additionally, activated carbon (AC) prepared from waste tyre material demonstrated a high chromium adsorption capability of 55.2 mg/g, while apple peel processed with modified H_3PO_4 showed a maximum chromium adsorption capacity of 36 mg/g [16]. Nevertheless, some studies have enriched the surface of activated carbon with functional groups using HNO_3, resulting in S_{BET} 1399 m^2/g and an increase in lactone functional groups [17]. With the addition of functional groups, such as –OH, –C=O, –P=O, –P–O–C, and numerous carbon-carbon bonds, the process of impregnating AC with H_3PO_4 also contributes to an increase in the BET-surface area (S_{BET}) of the resultant material to 1290 m^2/g [18]. These studies suggested that modifications to cellulose-based materials can enhance their adsorption capacity.

The hydrothermal carbonization (HTC) approach uses an aqueous solution and operates at 160–220°C, making it environmentally friendly, straightforward, and cost-effective [19, 20]. Biomass materials are optimal carbon sources for producing high-adsorption-capacity materials via HTC due to their renewability, high reactivity, and low cost. Lignocellulosic biomass, which consists mainly of glucose, can be efficiently carbonized via HTC to yield well-organized carbon spheres with a highly porous structure and a high surface area [21]. For example, a previous study reported a high S_{BET} of 1283 m^2/g and a micropore volume of 0.44 cm^3/g for glucose, obtained using a hydrothermal technique and KOH activation [22]. Acid modification, primarily using hydrochloric acid, nitric acid, or phosphoric acid, increases the S_{BET} of activated carbon, thereby enhancing its capacity to adsorb contaminants [23-25]. In one example, the adsorption performance was significantly enhanced after chemical activation with H_3PO_4; the mesopore volume and S_{BET} of orange peel-derived carbon increased from 0.025 cm^3/g and 117 m^2/g to 0.102 cm^3/g and 618 m^2/g, respectively [26].

The main objective of alkaline treatment (with substances like potassium hydroxide and sodium hydroxide) was to increase the number of functional groups containing oxygen and the specific surface area [27, 28]. For example, industrial alkali lignin was used to produce a hierarchical porous carbon-based adsorbent via combined hydrothermal and alkali activation for adsorbing Cr(VI) [26]. During KOH treatment, a few three-dimensional linked channels formed, and numerous active groups, including N- and O-containing ones, were generated. Hydrothermal carbon nanospheres were prepared from glucose and activated with aqueous NaOH. The outcomes showed that its surface, after impregnation with a NaOH solution, was enriched in –OH and –COOH groups, significantly altering its morphology, surface area, and pore volume [29]. Overall, modifying or activating carbon can be a useful method for producing adsorbents with high surface area and functional groups beneficial for adsorption.

This study aimed to investigate the influence of different chemical agents, including acrylic acid (AA), citric acid (CA), and H_2O_2, used to activate hydrochar derived from the hydrothermal process of glucose. The effects of bath operating parameters on the adsorption performance of the prepared materials were assessed, including pH, temperature, contact time, initial Cr(VI) concentration, and different background water sources. The adsorption mechanisms were elucidated using kinetic, thermodynamic, and adsorption isotherm models. Adsorption mechanisms associated with the removal of Cr(VI) from aqueous solutions were discussed herein.

2. Materials and methods

2.1. Reagents

In this study, glucose ($C_6H_{12}O_6$), potassium dichromate ($K_2Cr_2O_7$), sulfuric acid (H_2SO_4), sodium hydroxide (NaOH), hydrochloric acid (HCl), hydrogen peroxide (H_2O_2), citric acid ($C_6H_8O_7$), acrylic acid ($C_3H_4O_2$), and 1,5-diphenylcarbazide were obtained from Alpha Chemical Reagent Co., Ltd. (Tianjin, China). They were qualified as analytical grades. All working solutions used during all experiments were prepared by diluting chemicals in deionized water.

2.2. Preparation of materials

The materials were synthesized from glucose via hydrothermal, impregnation, and pyrolysis steps, as shown in Figure 1. Glucose hydrochar (GH) was produced by hydrothermal treatment of 32.4 g glucose and 120 mL deionized (DI) water in a Teflon-lined stainless steel autoclave at 190°C for 24 h [30]. GH was washed with alcohol (95%) and distilled water until the pH value was equal to that of the DI water.

Subsequently, 3.0 g HG was impregnated with 50 mL of each chemical agent, including H_2O_2, acrylic acid (AA), or citric acid (CA), with a concentration of 0.3 M at room temperature for 24 h. After that, the materials were washed and dried. The dried materials were then pyrolyzed at 900°C for 2 h under atmospheric conditions at a rate of 45°C/min and a flow rate of 0.5 L/min N_2. The materials were washed with DI water until the pH remained constant, then dried and sieved to a particle size of 0.088 mm. Four materials obtained, as described in Figure 1, will be compared in this study to clarify the influence of chemical agents on Cr(VI) adsorption in aqueous solution.

2.3. FT-IR analysis, pH_{PZC}, acidic and basic groups

Their surface morphology was displayed using scanning electron microscope (SEM) images (JSM-6510 LV; Japan). Fourier-transform infrared spectroscopy (FTIR; FT/IR-4600; Japan) was used to determine the main functional groups on their surface.

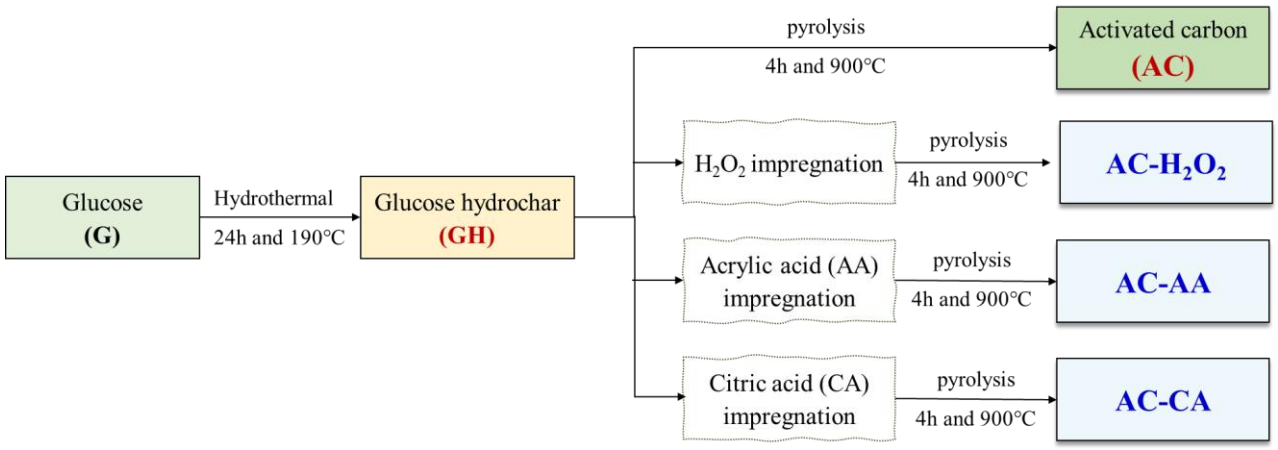

Fig. 1. Synthetic process of materials.

The drift method was used to estimate the pH at the material's point zero charge (pH_{PZC}) [23]. The acidic and basic groups on the adsorbent surfaces were determined by Boehm titration, using the technique described in the previous study, which quantifies carboxylic, phenolic, and lactonic functional groups in pristine and laden materials [30].

2.4. Adsorption and desorption experiments

The adsorption experiments were conducted in a batch reactor with a solid/liquid ratio of 0.5 g/L in a thermostatic shaker. The appropriate concentration of Cr(VI) solution was obtained by dissolving $K_2Cr_2O_7$ in DI water.

The diphenylcarbazide method was used to measure the concentration of Cr(VI) before and after the adsorption process [31]. Diphenylcarbazide formed a red-violet complex with Cr(VI), and the intensity of this complex was detected at 542 nm with a UV–vis spectrophotometer (Hitachi U-2910, Hitachi Corp., Japan). The total Cr concentration before and after adsorption was analyzed by atomic absorption spectroscopy (AAS; Hitachi ZA3300, Hitachi Corp., Japan).

The adsorption capacity of the materials was calculated by Eq. (1) at defined time intervals until reaching adsorption equilibrium after samples were taken and filtered through a 0.45-µm Whatman membrane filter.

$$q_e = \frac{(C_0 - C_e) \times V}{m} \quad (1)$$

where C_e (mg/L) is the total Cr concentration at equilibrium; C_0 (mg/L) is the initial concentration of total Cr; q_e (mg/g) is the adsorption capacity at equilibrium; V (L) is the volume of Cr solution; and m (g) is the mass of the adsorbent.

To investigate the influence of desorption taken by different extraction solutions, the laden adsorbent was shaken with 200 mL of various desorbing agents, including hot water at 60°C, NaOH (0.05 M), or HCl (0.05 M). The percentage of adsorbate desorbed (R_{Des}) from the laden adsorbent was calculated using Eq. (2).

$$R_{Des} = \frac{q_{e(2)}}{q_{e(1)}} \times 100\% \quad (2)$$

where $q_{e(1)}$ (mg/g) and $q_{e(2)}$ (mg/g) are the adsorption capacities of materials at the first and second cycles of adsorption and desorption, respectively.

2.5. Adsorption isotherms, kinetics, and thermodynamics

Three models were studied to investigate equilibrium parameters, including the Langmuir, Freundlich, and Redlich–Peterson models [32]. The Redlich–Peterson model was proposed to address the limitations of the Freundlich and Langmuir models. This model combines aspects of the Freundlich and Langmuir models and might be used to demonstrate adsorption equilibrium across a wide range of adsorbate concentrations [33]. Eqs. (3), (4), and (5) defined the Langmuir, Freundlich, and Redlich–Peterson models, respectively.

$$q_e = \frac{q_{max} K_L C_e}{1 + K_L C_e} \quad (3)$$

where q_{max} (mg/g) is the maximum adsorption capacity, and K_L is the Langmuir constant.

$$q_e = K_F C_e^{1/n} \quad (4)$$

where n is the adsorption intensity, and K_F (mg/g)/(mg/L)$^{1/n}$ is the Freundlich constant.

$$q_e = \frac{K_{RP} C_e}{1 + a_{RP} C_e^g} \quad (5)$$

where K_{RP} and a_{RP} (mg/L)$^{-g}$ are the Redlich–Peterson constants, and g is an exponent which must lie between 0 and 1.

Kinetic parameters were studied using the pseudo-first-order (PFO), pseudo-second-order (PSO), and Elovich models. The PFO, PSO, and Elovich models were defined as Eqs. (6), (7), and (8) [32, 33], respectively.

$$q_t = q_e (1 - e^{-k_1 t}) \quad (6)$$

$$q_t = \frac{q_e^2 k_2 t}{1 + k_2 q_e t} \quad (7)$$

where q_t (mg/g) is the adsorption capacity at contacting time t, and k_1 (1/min) and k_2 (g/(mg×min) are the PFO and PSO kinetic rate constants, respectively.

$$q_t = \frac{1}{\beta} \ln(t) + \frac{1}{\beta} \ln(\alpha\beta) \quad (8)$$

where α (mg/(g×min)) is the initial rate constant, and β (mg/g) is the desorption constant.

To investigate the effect of temperature on the adsorption process, the changes in standard enthalpy ($\Delta H°$), standard entropy ($\Delta S°$), and standard Gibbs energy ($\Delta G°$) were determined using Eqs. (9)–(12) [34].

$$\Delta G° = -RT \ln K_C \quad (9)$$

The following describes the relationship of $\Delta G°$ to $\Delta H°$ and $\Delta S°$:

$$\Delta G° = \Delta H° - T\Delta S° \quad (10)$$

$$\ln K_C = \left(\frac{-\Delta H°}{R}\right)\frac{1}{T} + \frac{\Delta S°}{R} \quad (11)$$

$$K_C = \frac{K_L}{\gamma_{Cr}} \times C^o \quad (12)$$

where K_c (dimensionless) is the adsorption equilibrium constant under the standard condition; K_L is the Langmuir constant (L/mol), $C°$ is the concentration of Cr at standard condition ($C°$= 1 mol/L); γ_{Cr} is the activity coefficient of Cr and it approaches unity under dilute conditions; R is the universal gas constant (8.3144 J/(mol×K)); and T (K) is the solution temperature in Kelvin.

All experiments were conducted in triplicate. The reported results represent the average values of the three independent measurements.

3. Results and discussion

3.1. SEM, FTIR, and pH_{PZC} analysis of the materials

The SEM image (Figure 2a) reveals interconnected spheres with smooth outer surfaces, regular spherical shapes, consistent diameters, and high purity.

The FTIR spectra of spherical activated carbon materials demonstrated the typical characteristics of the adsorbents (Figure 2b). The stretching vibrations in the (–OH) hydroxyl groups of hemicellulose, cellulose, and lignin are responsible for the bands at 3700–3000 cm^{-1} [35]. The bands at 1800–1650 cm^{-1} indicate the presence of carboxylic and lactonic groups (C=O) [36]. The C=C double bonds in aromatic rings are likely responsible for the bands in the region between 1650 and 1480 cm^{-1}. The stretched C–O groups are observed in bands between 1290 and 970 cm^{-1} [39]. Lastly, the bands in the 970–730 cm^{-1} range, associated with the aromatic C–H out-of-plane bending mode, are characteristic of aromatic benzene rings [37, 38].

Notably, the intensities of the –OH, C–H, C=O, and C–O peaks in AC-AA and AC-CA (Figure 2b) were higher than those in AC, indicating that impregnation with acrylic acid and citric acid can increase the abundance of these functional groups. Previous research indicated that these groups are features of the carboxylic functional group and are effective at removing Cr(VI) [40].

The point of zero charge (PZC) was a defining characteristic of the electrical state of adsorbent surfaces in solution. The value of pH_{PZC} refers to the pH level at which an adsorbent's net (internal and external) surface charge is zero. The plot and pH_{PZC} values of adsorbent samples obtained using the pH drift method are shown in Figure 2c. The pH_{PZC} of the materials followed the order: AC (7.10) > AC-H_2O_2 (6.98) > AC-AA (5.89) > AC-CA (5.58), indicating that the chemical modification

significantly influenced the adsorbent's pH_{PZC} values and the surface charge characteristics of the adsorbents.

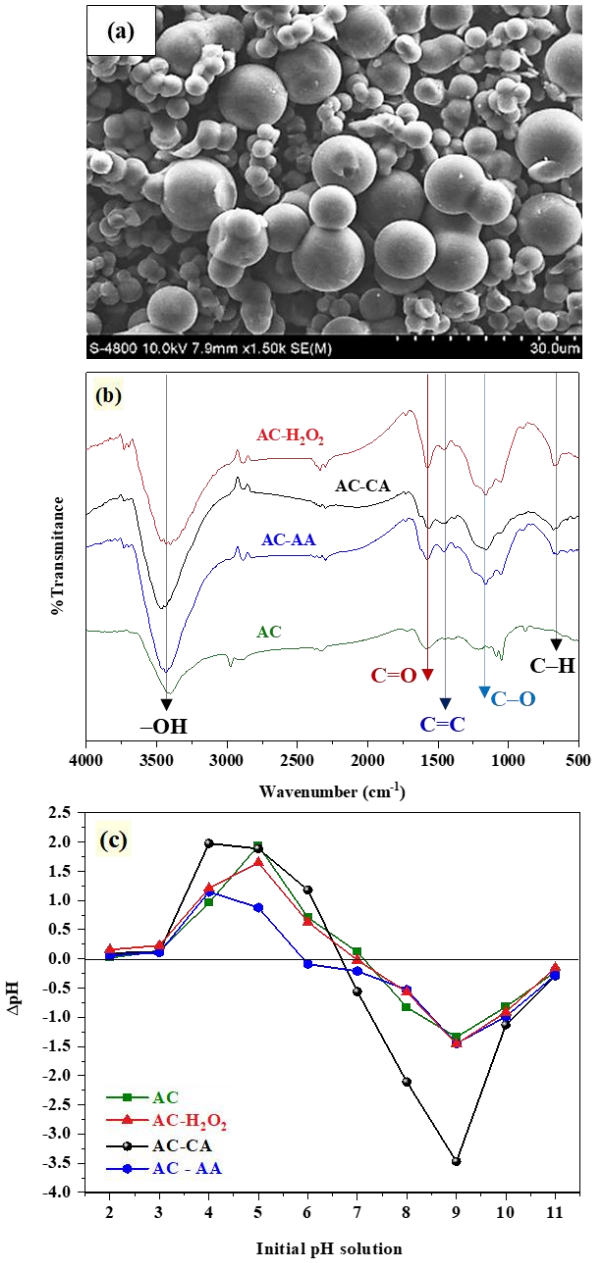

Fig. 2. SEM image of (a) AC, (b) FTIR analysis, and (c) pH_{PZC} analysis of materials.

3.2. Acidic and basic groups of materials

The results of qualifying three common functional groups in synthesized materials before and after adsorption are presented in Table 1.

The results showed that total functional groups measured before adsorption of AC-AA were the highest with 4.02 (mmol/g), followed by AC-CA (3.61 mmol/g), and AC-H_2O_2 (2.47 mmol/g); the lowest was AC with 1.54 mmol/g. These findings indicate that chemical modification effectively increased the functional group content of the materials, even after pyrolysis at 900℃ after impregnation, in agreement with the FTIR results (Figure 2b). The results also indicated that impregnating the materials with AA, CA, and H_2O_2 can at least double the carboxylic group content while reducing the phenolic group content.

In addition, impregnating GH in AA, CA, and H_2O_2 increased lactonic groups approximately 13, 15, and 4 times, respectively, compared to AC. Among the three functional groups, the carboxylic group exhibited the highest surface content, which may facilitate the adsorption of Cr(VI) and Cr(III) via complexation [41]. The lactonic group has been reported as a key functional group for removing Cr(VI) from water [42]. Furthermore, Table 1 shows that impregnation of GH into AA and CA effectively enhanced the surface carboxylic and lactonic groups on the AC samples. The reduction of these functional groups after adsorption implies that they play a vital role in the adsorption of Cr(VI) in water.

Table 1. Quantification of functional groups in synthesized materials before and after adsorption.

Adsorbent	Before adsorption (mmol/g)				After adsorption (mmol/g)			
	Carboxylic	Phenolic	Lactonic	Total	Carboxylic	Phenolic	Lactonic	Total
AC	1.05	0.41	0.08	1.54	0.22	0.14	~0	0.36
AC-CA	2.09	0.34	1.18	3.61	0.67	0.16	0.13	0.96
AC-AA	2.89	0.11	1.02	4.02	0.94	0.05	0.17	1.16
AC-H_2O_2	2.12	0.04	0.31	2.47	0.49	~0	0.18	0.67

3.3. Effect of pH solution and time on Cr(VI) adsorption

The pH of the solution is one of the most important parameters influencing heavy metal ion adsorption from aqueous solutions, as it directly affects the adsorbent surface charge density and the speciation of the metal ions in solution [23].

The effect of solution pH on Cr(VI) adsorption by adsorbent materials is shown in Figure 3a. The removal of Cr(VI) from an aqueous solution is highly dependent on pH, with maximal adsorption at pH 2.0. The speciation of Cr(VI) in aqueous solution at various pH values includes different anion forms, including H_2CrO_4, $HCrO_4^-$, CrO_4^{2-}, and $Cr_2O_7^{2-}$ [43]. In the pH range of 2.0– 6.0, $HCrO_4^-$ and $Cr_2O_7^{2-}$ are predominantly in equilibrium; while $HCrO_4^-$ dominates in solution at pH 2. As the pH increases, $HCrO_4^-$ transforms to a chromate ion (CrO_4^{2-}) [44]. During adsorption, a chromate ion (CrO_4^{2-}) requires two active sites, whereas an $HCrO_4^-$ ion requires only one active site. As a result, $HCrO_4^-$ was more readily adsorbed on the carbon surfaces [23]. The enhanced adsorption of activated carbon at low pH may be attributed to the high concentration of H^+ ions, which neutralise the negatively charged adsorbent surface, thereby reducing electrostatic hindrance to chromate ion diffusion [45].

As presented in Figure 2c, the pH_{PZC} values of all materials ranged from 5.58 to 7.1, implying that when the solution pH decreases below these values, the surface of materials became more positively charged, thereby enhancing electrostatic attraction toward negatively charged Cr(VI) species [46, 47]. Consequently, the highest adsorption capacity of Cr(VI) onto the adsorbent surface was observed at the lowest pH = 2 (Figure 3a) [43].

The influence of contact time on adsorption capacity is shown in Figure 3b. The results indicate that the adsorption rate rapidly increased until 180 min, then increased slightly until equilibrium was reached at approximately 480 min. Figure 3b also shows that the chemically modified activated carbons exhibited higher adsorption rates than the unmodified AC, leading to higher adsorption capacities.

These results might be attributed to the higher abundance of functional groups in the chemically modified activated carbons, which play a crucial role in Cr(VI) removal [48]. The findings suggest that chemical modification significantly enhances AC's adsorption efficiency. Compared with previous studies, the equilibrium period of 180–360 min for these adsorbents is relatively short. For example, the equilibrium duration of modified activated carbon created from olive bagasse was 10 h [49], while charcoal produced from sawdust attained equilibrium in 5 h [50], and activated carbon synthesized from waste lignocellulosic material required 360 min to reach equilibrium [51]. This indicates that the chemically modified activated carbon employed in this study has a higher adsorption capacity and attains equilibrium more rapidly, underscoring its potential for efficient, time-effective Cr(VI) removal.

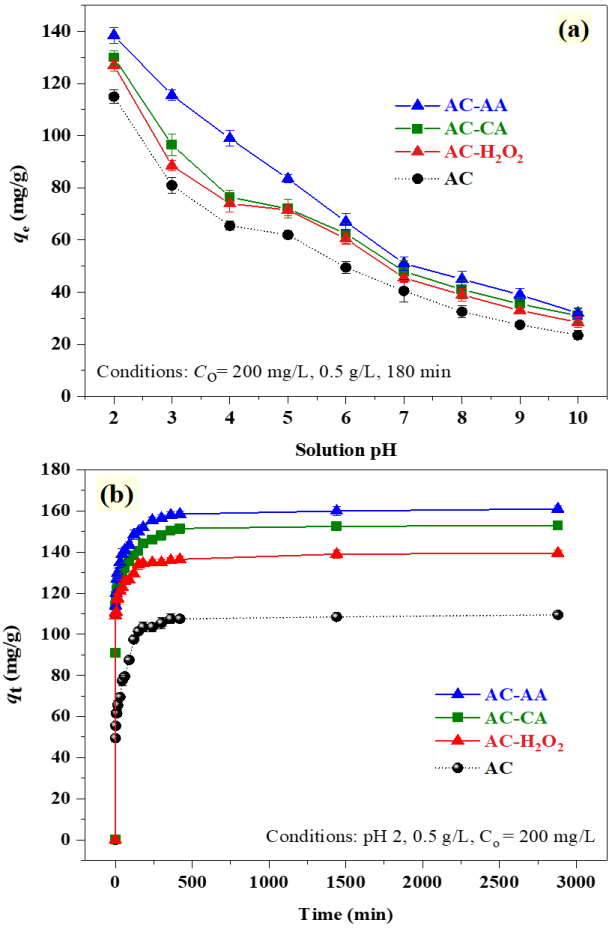

Fig. 3. Influences of (a) the solution pH and (b) contact time.

3.4. Adsorption isotherm

Figure 4 shows the best-fit results for the kinetic data using three common adsorption isotherm

models. The Langmuir and the Freundlich models are the most common adsorption isotherms, based on different assumptions about adsorption processes. The Redlich–Peterson model, a hybrid model of these two models [52-53]. As illustrated in Figure 4, the Redlich–Peterson model best fits the experimental data. Furthermore, the *g* value is close to 1 (Table S1), suggesting a better fit of the experimental data with the Langmuir model compared to the Freundlich model [54-56].

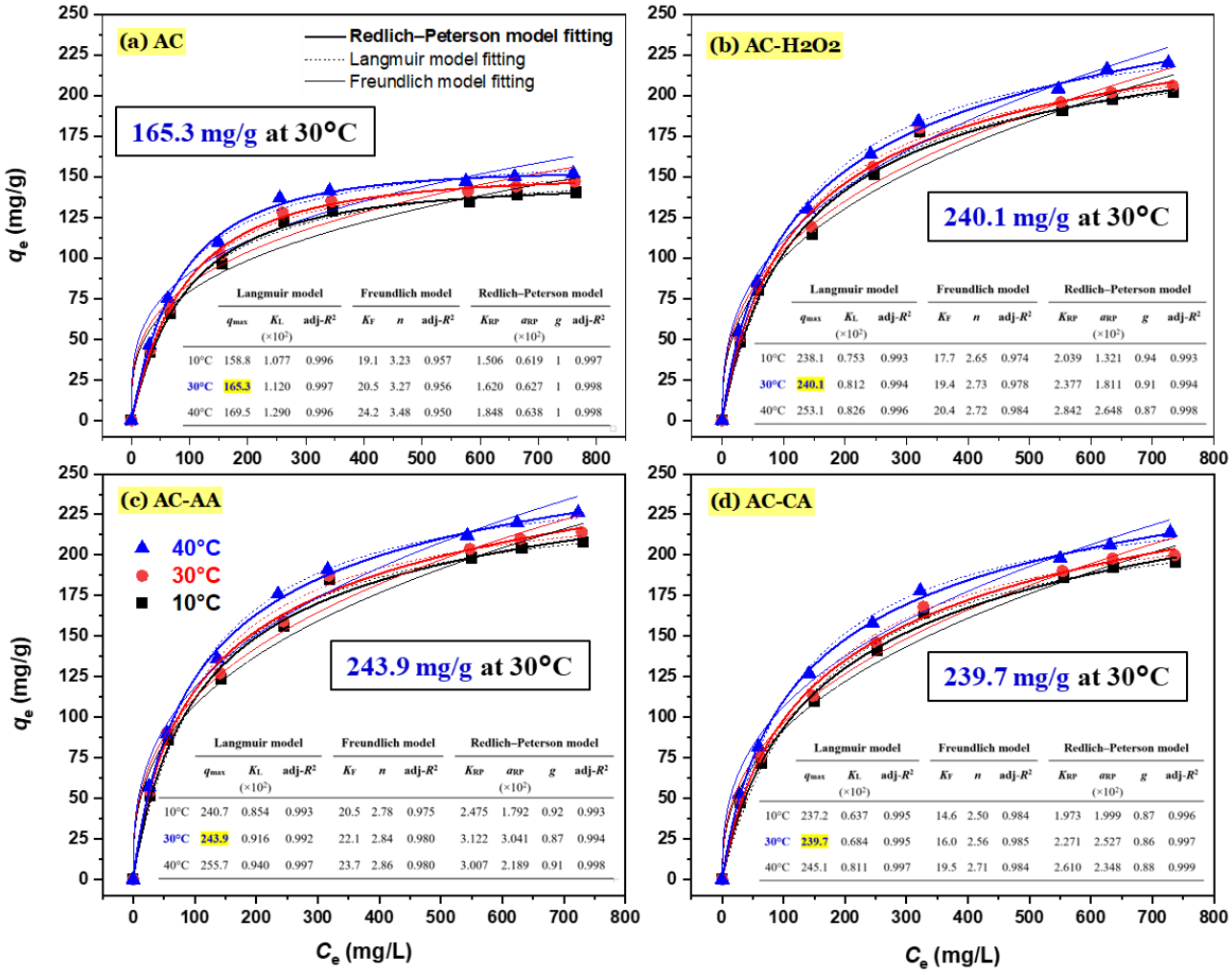

Fig. 4. Adsorption isotherms parameters of adsorbent materials for Cr(VI) adsorption of (a) AC, (b) AC-H_2O_2, (c) AC-AA, and (d) AC-CA.

The maximum adsorption capacity predicted by the Langmuir model was 165.3 mg/g, lower than that of AC-AA (243.9 mg/g), AC-H_2O_2 (240.1 mg/g), and AC-CA (239.7 mg/g). The higher maximum adsorption capacities of chemically modified ACs compared to pristine AC can be explained by two main reasons: (1) enhanced electrostatic interactions between the adsorbent and adsorbate, as evidenced by the pH effect experiment (Figure 3a); and (2) the increased abundance of surface functional groups on the modified materials. The enhanced adsorption performance of AC-AA may be attributed to the introduction of oxygen-containing functional groups (–COOH), which enhance surface polarity and provide additional interaction sites for interaction with Cr(VI) species [57].

When comparing the maximum adsorption capacities (Table S2), all materials had capacities much higher than those reported in other studies, such as corn straw (176 mg/g), nanotubes (85.8 mg/g), and apple peels (36 mg/g). The results showed that the adsorption capacities of the materials synthesized in this study were superior to those of the reported materials, even exceeding those of materials synthesized by more complex

modification processes, such as nanotubes, or by using more chemicals, which pose greater environmental risks.

3.5. *Adsorption kinetics*

Figure 5 illustrates the results of fitting the kinetic data to the PFO, PSO, and Elovich models using four adsorbents. All parameters obtained from all adsorbents exhibited a better fit to the Elovich model ($R^2 > 0.95$) than to the PFO and PSO models. Previous investigations indicated a similar observation [58-59]. Furthermore, the high α value of the Elovich model obtained for three chemically modified materials indicates that their surfaces are highly heterogeneous [60-63, 64], which might facilitate adsorption and yield high adsorption capacities [57, 65, 66].

3.6. *Adsorption thermodynamics*

Table 2 shows the negative values of $\Delta G°$ and positive values of $\Delta H°$ for the adsorption processes of all materials, indicating that the adsorption process is thermally favourable and endothermic. Adsorption is influenced by temperature and depends on the mobility of heavy metal ions [67]. The adsorption of Cr(VI) on the synthesized materials was endothermic, meaning that heat was absorbed as the reaction progressed. The positive value of $\Delta S°$ indicates an increase in reaction irregularity at the solid-liquid interface [68].

The $\Delta H°$ values of the adsorption processes were low (2.34–5.37 kJ/mol). In general, chemisorption are associated with much higher $\Delta H°$ (typically ≥200 kJ/mol) [34]. Therefore, the adsorption of Cr(VI) onto the prepared materials was predominantly governed by physical adsorption, characterised by relatively weak adsorption interactions.

3.7. *Desorption experiments*

The results in Figure 6 indicated that NaOH is the most efficient desorption agent among the three tested, whereas HCl and hot water at 60°C show comparatively lower effectiveness in releasing chromium. The use of HCl and hot water solutions is particularly ineffective in desorbing chromium.

At pH values below the pHpzc, the adsorbent surface carries a positive charge. This promotes electrostatic attraction between the surface and OH^- ions from the NaOH solution, leading to the displacement of adsorbed $HCrO_4^-$ ions into the surrounding environment. Conversely, at pH levels higher than pH_{pzc}, the adsorbent surface becomes negatively charged, while Cr(VI) primarily exists as CrO_4^{2-} under alkaline conditions. Under these circumstances, the desorption of Cr(VI) is facilitated through the exchange of CrO_4^{2-} ions with OH^- ions. Notably, the experiments demonstrated that approximately 70% of Cr(VI) could be desorbed using NaOH, indicating that electrostatic forces play a key role in the adsorption of Cr(VI) [69-71]. In this case, because the adsorbent surface was positively charged, the use of a basic solution effectively promoted competition between OH^- and $HCrO_4^-$ anions, resulting in efficient desorption.

Table 2. Thermodynamic parameters for the Cr(VI) adsorption by the adsorbent materials.

Materials	Temperature (K)	$\Delta G°$ (kJ/mol)	$\Delta H°$ (kJ/mol)	$\Delta S°$ (J/(mol×K))
AC	283	–14.89	3.93	66.35
	303	–16.04		
	313	–16.94		
AC-H_2O_2	283	–14.05	2.34	57.93
	303	–15.23		
	313	–15.78		
AC-AA	283	–14.34	2.38	59.10
	303	–15.53		
	313	–16.11		
AC-CA	283	–13.65	5.37	67.06
	303	–14.80		
	313	–15.73		

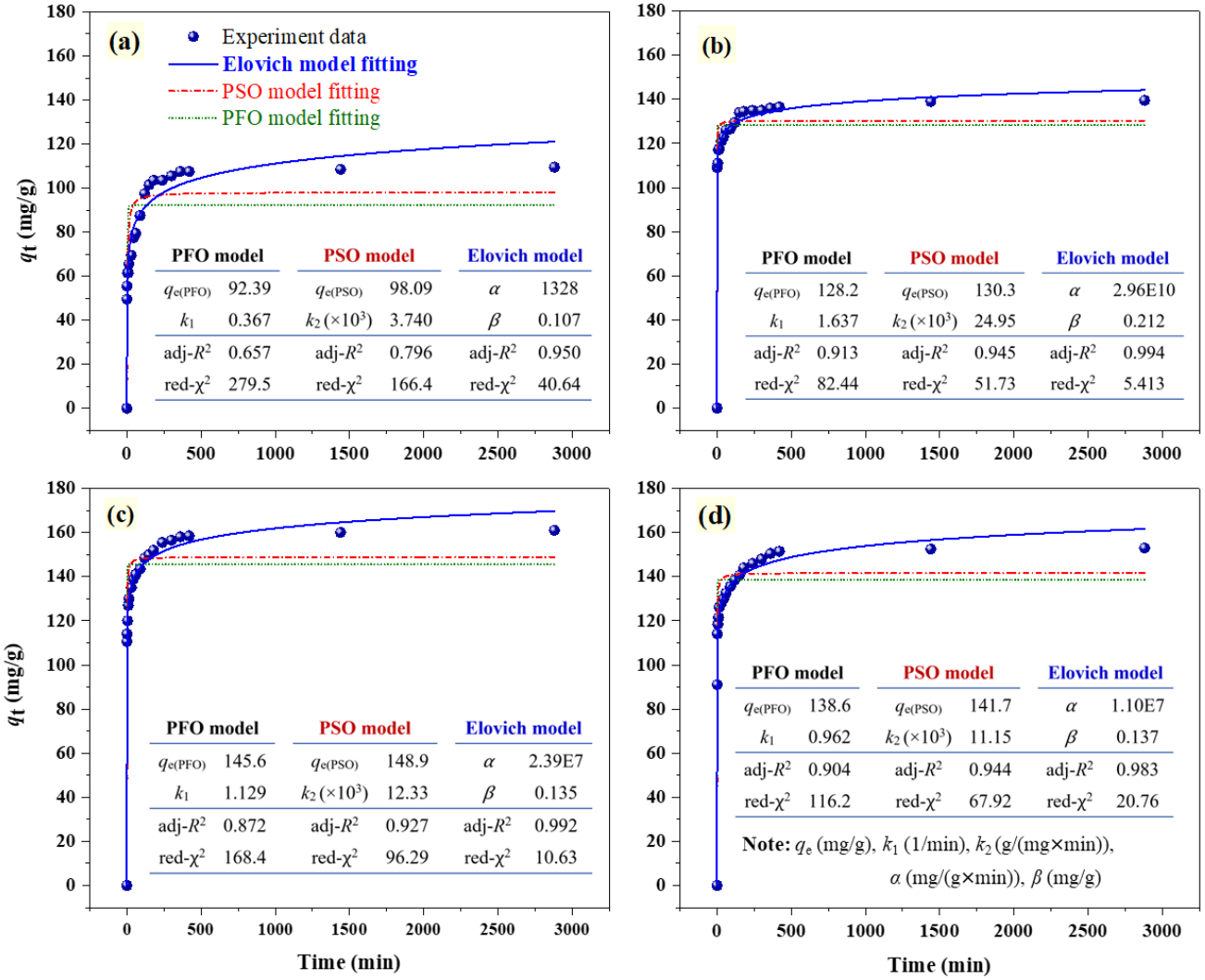

Fig. 5. Kinetic parameters for Cr(VI) adsorption by the adsorbent materials: (a) AC, (b) AC-H_2O_2, (c) AC-AA, and (d) AC-CA.

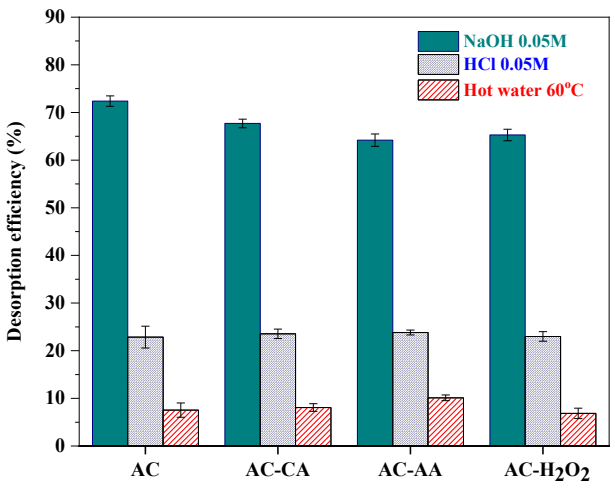

Fig. 6. Desorption efficiency of Cr(VI) on the adsorbents.

Both methods have significant limitations when using HCl and hot water at 60°C for chromium desorption. HCl creates an acidic environment that facilitates chromium desorption, but its efficiency is hindered because chromium typically exists as Cr^{3+} or forms insoluble complexes under these conditions, thereby hindering its complete release from the adsorbent surface. Furthermore, HCl cannot oxidise chromium to the more soluble Cr(VI) form, thereby limiting desorption. Hot water exhibits the lowest desorption efficiency among the methods. As the temperature increases, thermal energy intensifies molecular vibrations, enhancing interactions between water molecules and the adsorbent surface [72]. This thermal agitation is sufficient only to disrupt weak physical interactions, leading to the partial release of

adsorbed ions into solution. These findings indicate that weak forces, such as van der Waals interactions, contribute to the adsorption mechanisms of all materials.

3.8. Effect of NaCl concentrations and water matrices

Wastewater from various industries contains various salts, which can increase ionic strength and negatively affect adsorption [73]. The research results presented in Figure 7a showed that the chromium adsorbent solution's adsorption capacity varied when NaCl was added, significantly influencing the chromium adsorption capacity of the adsorbent. Chromium adsorption on the adsorbent was slower in the presence of Cl^- ions. In comparison, with the absence of Cl^-, the concentration of Cl^- increased from 0.01 M to 1 M. This phenomenon can be explained by several factors. First, at pH 2, the positively charged adsorbent surface promoted competition between Cl^- and $HCrO_4^-$ ions for available adsorption sites, leading to a gradual decrease in adsorption capacity with increasing Cl^- concentration.

Because the higher the concentration of NaCl, the more Cl^- ions were present in the solution, increasing the competition with $HCrO_4^-$ in the adsorption process. Second, high NaCl concentrations may increase the solution's ionic strength, thereby affecting the Cr(VI) activity coefficient and significantly reducing collision and contact between the sorbent [74]. Lastly, the adsorbent species in solution come into contact with the solid adsorbent. An electrically diffused double layer encircles these species, and the addition of NaCl noticeably increases its thickness. Due to a decrease in electrostatic attraction caused by this expansion, the amount of Cr(VI) ions that may be adsorbed is also reduced. This expansion prevents the adsorbent particles and Cr(VI) species from interacting intimately [75].

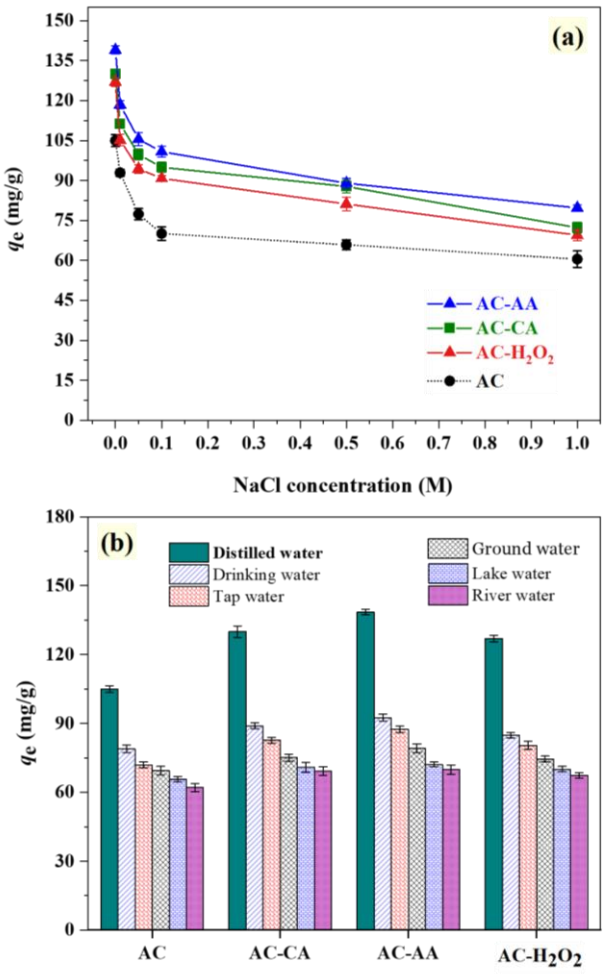

Fig. 7. Effect of (a) NaCl concentrations and (b) different water sources on adsorption capacity (Experimental conditions: C_o = 200 mg/L, 3 h, pH 2, solid/liquid ratio 0.5 g/L, and room temperature).

The adsorption process was significantly impacted by substances from water sources (Figure 7b). For all materials, the adsorption capacity decreased in the following order: distilled water > drinking water > tap water > ground water > lake water > river water. The order in which this adsorbent's adsorption capacity was reduced corresponds exactly to the quality of the water: distilled water > drinking water > tap water > groundwater > lake water > river water. The results showed that dissolved substances in aqueous environments exerted a significant competitive influence, reducing adsorption capacity in particular water environments. The higher the water quality, the greater the ion competition. An insignificant amount of $HCrO_4^-$ was present in water that contained ions. On the contrary, the concentrations of different ions in the water source

increase with reduced water quality, thereby increasing competition with $HCrO_4^-$ in lake and river water.

3.9. *Proposed adsorption mechanisms*

Hexavalent and trivalent chromium may coexist in the solution and on the adsorbent after the Cr(VI) adsorption procedure if the reduction of Cr(VI) to Cr(III) takes place. Many researchers have examined errors in analyzing chromium species in aqueous environments (liquid phase) and on the loaded adsorbent (solid phase) following the Cr(VI) adsorption procedure [76]. Basically, atomic absorption spectroscopy (AAS) is used to determine the total (trivalent and hexavalent) chromium in solution [44]. The reduction of Cr(VI) under acidic conditions may be partially attributed to electron-donating surface functionalities, particularly phenolic groups. As shown in Figure 8, the reduction rate of Cr(VI) increased with decreasing solution pH because protons participate directly in the reduction process [78].

Cr(VI) removal at low pH may also occur through two indirect mechanisms [33]. In the first mechanism, electron-donating functional groups on the adsorbent surface interact with Cr(VI) species in solution, reducing the highly toxic Cr(VI) to the less toxic Cr(III). This reduction is thermodynamically favourable because Cr(VI) has a high oxidation potential (typically greater than +1.35 V).

According to the literature, Cr(VI) oxyanions can be spontaneously reduced to Cr(III) upon interaction with electron-donating groups such as hydroxyl groups on the adsorbent surface [44]. Oxygen-containing functional groups on the material surface provide the electrons involved in the reduction process described in Eq. (13). The second mechanism includes a three-step procedure: (i) electrostatic attraction between Cr(VI) anions and positively charged groups on the adsorbent surface; (ii) reduction of Cr(VI) to Cr(III) by neighboring electron-donating functional groups; and (iii) either release of Cr(III) cations into the aqueous phase due to electrostatic repulsion or complexation of Cr(III) with adjacent surface functional groups.

Based on the proposed mechanisms and experimental results, the adsorbents primarily adsorbed Cr(VI) species. However, previous studies have shown that a portion of the adsorbed Cr(VI) anions can be reduced to Cr(III) cations during adsorption. In this reduction reaction, the abundant hydroxyl groups on the surface of the activated carbon serve as electron-donating functional groups.

$$HCrO_4^- + 7H^+ + 3e^- \rightleftharpoons Cr^{3+}\ 4H_2O\ (E^o = +1.35V) \quad (13)$$

Adsorbents with high surface areas can enhance adsorption by providing more active sites for chromium interaction, particularly within the pore structure. The adsorption of chromium onto the synthesized materials mainly occurs on the adsorbent surface. In addition, at low pH (< pH_{PZC}), the material's surface will carry a positive charge, mainly due to the OH_2^+ groups present on its surface. Therefore, there is an electrostatic attraction between the OH_2^+ groups and Cr(VI) anions in solutions. This electrostatic interaction is considered one of the major mechanisms contributing to chromium removal in the present study.

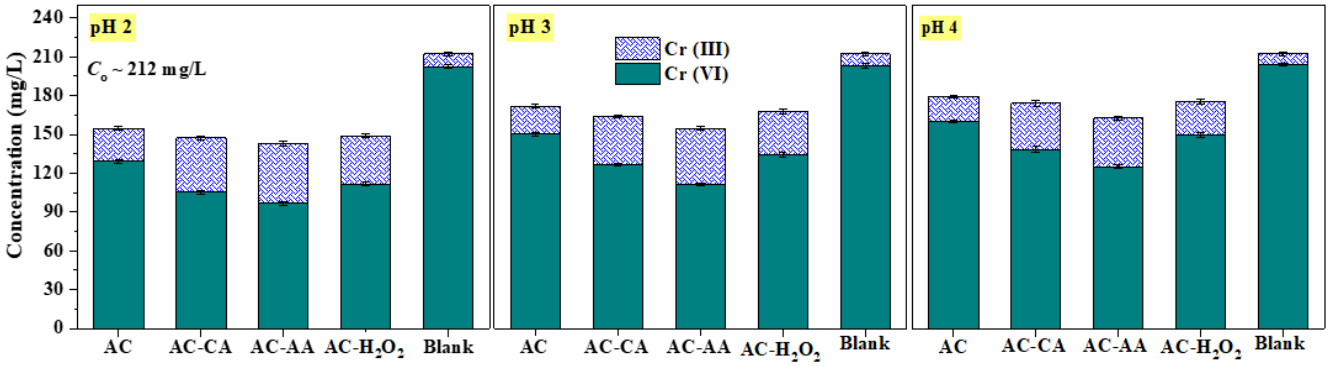

Fig. 8. Concentrations of Cr(VI) and Cr(III) in solutions after adsorption at different pH values.

4. Conclusions

Spherical hydrochar-derived activated carbons were successfully synthesized through hydrothermal carbonization of glucose, chemical impregnation, and pyrolysis. Chemical modification with H_2O_2, citric acid, and acrylic acid significantly increased the abundance of oxygen-containing functional groups and enhanced the adsorption performance toward Cr(VI). Among the synthesised materials, AC-AA exhibited the highest adsorption capacity (243.9 mg/g), surpassing those of many previously reported adsorbents. The adsorption process was strongly dependent on solution pH and was most effective at pH 2 due to enhanced electrostatic attraction between the adsorbent surface and Cr(VI) anions. Kinetic and thermodynamic studies indicated that the adsorption process followed the Elovich model and was endothermic. The adsorption mechanisms mainly involved electrostatic interaction, surface complexation, and partial reduction of Cr(VI) to Cr(III). The results demonstrate that chemical impregnation before pyrolysis is an effective strategy for producing high-performance adsorbents for Cr(VI) removal from aqueous solutions.

Acknowledgements

The authors would like to express their gratitude to Ms Nguyen Thi Phuong and Ms Nguyen Thi Cam Vi for their assistance in conducting the experiments.

Author's contribution

Conceptualization: Nguyen Duy Dat, Hai Nguyen Tran; Methodology: Nguyen Duy Dat; Formal analysis and investigation: Nguyen Duy Dat, Quang Sang Huynh; Validation and software: Hai Nguyen Tran; Writing - original draft preparation: Quang Sang Huynh, Nguyen Duy Dat; Writing - review and editing: Nguyen Duy Dat, My Linh Nguyen, Hai Nguyen Tran; Supervision: Nguyen Duy Dat.

Conflict of interest

The authors reported no potential conflict of interest.

Data availability

The datasets generated and/or analyzed during the current study are available from the corresponding author on reasonable request.

Funding

Self-funded.

Declaration of Using Generative AI

Generative AI was used solely for language editing and to improve the manuscript's readability. The authors used Grammarly to improve the English language and grammar of this work. The authors take full responsibility for the content, interpretation, and accuracy of the manuscript.

References

[1] Dat, N. D., Nguyen, L. S. P., Vo, T.-D.-H., Van Nguyen, T., Do, T. T. L., Tran, A. T. K., & Hoang, N. T.-T. (2023). Pollution characteristics, associated risks, and possible sources of heavy metals in road dust collected from different areas of a metropolis in Vietnam. *Environmental Geochemistry and Health*, *45*, 7889-7907. https://doi.org/10.1007/s10653-023-01696-4

[2] Dat, N. D., Huynh, Q. S., Tran, K. A. T., & Nguyen, M. L. (2023). Performance of heterogeneous Fenton catalyst from solid wastes for removal of emerging contaminant in water: A potential approach to circular economy. *Results in Engineering*, *18*, 101086. https://doi.org/10.1016/j.rineng.2023.101086

[3] Cataldo, E., Salvi, L., Paoli, F., Fucile, M., Masciandaro, G., Manzi, D., Masini, C. M., & Mattii, G. B. (2021). Application of zeolites in agriculture and other potential uses: A review. *Agronomy*, *11*, 1547. https://doi.org/10.3390/agronomy11081547

[4] Valentín-Reyes, J., García-Reyes, R., García-González, A., Soto-Regalado, E., & Cerino-Córdova, F. (2019). Adsorption mechanisms of hexavalent chromium from aqueous solutions on modified activated carbons. *Journal of Environmental Management*, *236*, 815-822. https://doi.org/10.1016/j.jenvman.2019.02.014

[5] Dhar, P. K., Naznin, A., & Hosna Ara, M. (2020). Health risks assessment of heavy metal

contamination in drinking water collected from different educational institutions of Khulna City Corporation, Bangladesh. *Advances in Environmental Technology*, *4*, 235–250.

[6] Ali, H., Khan, E., & Ilahi, I. (2019). Environmental chemistry and ecotoxicology of hazardous heavy metals: Environmental persistence, toxicity, and bioaccumulation. *Journal of Chemistry*, *2019*, 6730305. https://doi.org/10.1155/2019/6730305

[7] den Braver-Sewradj, S. P., van Benthem, J., Staal, Y. C., Ezendam, J., Piersma, A. H., & Hessel, E. V. (2021). Occupational exposure to hexavalent chromium. Part II. Hazard assessment of carcinogenic effects. *Regulatory Toxicology and Pharmacology*, *126*, 105045. https://doi.org/10.1016/j.yrtph.2021.105045

[8] Boosaeidi, N., Pourkhabbaz, A., & Jahani, M. (2017). Biosorption of hexavalent chromium by the agricultural wastes of the cotton and barberry plants. *Advances in Environmental Technology*, *3*(3), 159–167. https://doi.org/10.22104/aet.2017.579

[9] Achmad, R. T., & Auerkari, E. I. (2017). Effects of chromium on human body. *Annual Research & Review in Biology*, *13*, 1-8. https://doi.org/10.9734/ARRB/2017/33462

[10] World Health Organization. (2020). *Chromium in drinking-water*. World Health Organization.

[11] Sinduja, M., Sathya, V., Maheswari, M., Dhevagi, P., Kalpana, P., Dinesh, G., & Prasad, S. (2022). Evaluation and speciation of heavy metals in the soil of the sub urban region of Southern India. *Soil and Sediment Contamination*, *31*, 974-993. https://doi.org/10.1080/15320383.2022.2030298

[12] Velusamy, S., Roy, A., Sundaram, S., & Kumar Mallick, T. (2021). A review on heavy metal ions and containing dyes removal through graphene oxide-based adsorption strategies for textile wastewater treatment. *The Chemical Record*, *21*, 1570-1610. https://doi.org/10.1002/tcr.202000153

[13] Phạm, H. G., & Do, Q. H. (2016). Removing Heavy Metals in Water by Sorption using Phosphoric Acid Modified Rice Straw. VNU *Journal of Science: Earth and Environmental Sciences*, *32*(1). https://js.vnu.edu.vn/EES/article/view/2686

[14] Vo, A. T., Nguyen, V. P., Ouakouak, A., Nieva, A., Doma Jr, B. T., Tran, H. N., & Chao, H.-P. (2019). Efficient removal of Cr(VI) from water by biochar and activated carbon prepared through hydrothermal carbonization and pyrolysis: Adsorption-coupled reduction mechanism. *Water*, *11*, 1164. https://doi.org/10.3390/w11061164

[15] Ma, H., Yang, J., Gao, X., Liu, Z., Liu, X., & Xu, Z. (2019). Removal of chromium(VI) from water by porous carbon derived from corn straw: Influencing factors, regeneration and mechanism. *Journal of Hazardous Materials*, *369*, 550-560. https://doi.org/10.1016/j.jhazmat.2019.02.063

[16] Enniya, I., Rghioui, L., & Jourani, A. (2018). Adsorption of hexavalent chromium in aqueous solution on activated carbon prepared from apple peels. *Sustainable Chemistry and Pharmacy*, *7*, 9-16. https://doi.org/10.1016/j.scp.2017.11.003

[17] Demiral, İ., Samdan, C., & Demiral, H. (2021). Enrichment of the surface functional groups of activated carbon by modification method. *Surfaces and Interfaces*, *22*, 100873. https://doi.org/10.1016/j.surfin.2020.100873

[18] Danish, M., Pin, Z., Ziyang, L., Ahmad, T., Majeed, S., Yahya, A. N. A., Khanday, W. A., & Khalil, H. A. (2022). Preparation and characterization of banana trunk activated carbon using H3PO4 activation: A rotatable central composite design approach. *Materials Chemistry and Physics*, *282*, 125989. https://doi.org/10.1016/j.matchemphys.2022.125989

[19] Li, D., Guo, Y., Li, Y., Liu, Z., & Chen, Z. (2022). Waste-biomass tar functionalized carbon spheres with N/P Co-doping and hierarchical pores as sustainable low-cost energy storage materials. *Renewable Energy*, *188*, 61-69. https://doi.org/10.1016/j.renene.2022.01.109

[20] An, Q., Wang, Q., & Zhai, J. (2024). Hydrothermal carbonization of corncob for hydrochar production and its combustion reactivity in a blast furnace. *Environmental Science and Pollution Research*, *31*, 16653-16666. https://doi.org/10.1007/s11356-024-32242-z

[21] Nizamuddin, S., Baloch, H. A., Griffin, G. J., Mubarak, N. M., Bhutto, A. W., Abro, R., Mazari, S. A., & Ali, B. S. (2017). An overview of effect of process parameters on hydrothermal carbonization of biomass. *Renewable and Sustainable Energy Reviews*, *73*, 1289-1299. https://doi.org/10.1016/j.rser.2016.12.122

[22] Li, M., Li, W., & Liu, S. (2011). Hydrothermal synthesis, characterization, and KOH activation of carbon spheres from glucose. *Carbohydrate Research*, *346*, 999-1004. https://doi.org/10.1016/j.carres.2011.03.020

[23] Kumar, A., & Jena, H. M. (2017). Adsorption of Cr(VI) from aqueous solution by prepared high surface area activated carbon from Fox nutshell by chemical activation with H3PO4. *Journal of Environmental Chemical Engineering*, *5*, 2032-2041. https://doi.org/10.1016/j.jece.2017.03.035

[24] Liu, X., He, C., Yu, X., Bai, Y., Ye, L., Wang, B., & Zhang, L. (2018). Net-like porous activated carbon materials from shrimp shell by solution-processed carbonization and H3PO4 activation for methylene blue adsorption. *Powder Technology*, *326*, 181-189. https://doi.org/10.1016/j.powtec.2017.12.034

[25] Shi, Y., Liu, G., Wang, L., & Zhang, H. (2019). Activated carbons derived from hydrothermal impregnation of sucrose with phosphoric acid: Remarkable adsorbents for sulfamethoxazole removal. *RSC Advances*, *9*, 17841-17851. https://doi.org/10.1039/C9RA02610J

[26] Wang, Y., Xu, Y., Lu, X., Liu, K., Li, F., Wang, B., Wang, Q., Zhang, X., Yang, G., & Chen, J. (2023). Biomass-based hydrothermal carbons for the contaminants removal of wastewater: A mini-review. *International Journal of Molecular Sciences*, *24*, 1769. https://doi.org/10.3390/ijms24021769

[27] Bedin, K. C., Martins, A. C., Cazetta, A. L., Pezoti, O., & Almeida, V. C. (2016). KOH-activated carbon prepared from sucrose spherical carbon: Adsorption equilibrium, kinetic and thermodynamic studies for methylene blue removal. *Chemical Engineering Journal*, *286*, 476-484. https://doi.org/10.1016/j.cej.2015.10.099

[28] Kim, D.-W., Kil, H.-S., Nakabayashi, K., Yoon, S.-H., & Miyawaki, J. (2017). Structural elucidation of physical and chemical activation mechanisms based on the microdomain structure model. *Carbon*, *114*, 98-105. https://doi.org/10.1016/j.carbon.2016.11.082

[29] Zhang, P., Qiao, Z.-A., & Dai, S. (2015). Recent advances in carbon nanospheres: Synthetic routes and applications. *Chemical Communications*, *51*, 9246-9256. https://doi.org/10.1039/C5CC01759A

[30] Tran, H. N., Lee, C.-K., Nguyen, T. V., & Chao, H.-P. (2018). Saccharide-derived microporous spherical biochar prepared from hydrothermal carbonization and different pyrolysis temperatures: Synthesis, characterization, and application in water treatment. *Environmental Technology*, *39*, 2747-2760. https://doi.org/10.1080/09593330.2017.1365941

[31] Schumacher, P., Fischer, F., Sann, J., Walter, D., & Hartwig, A. (2022). Impact of nano- and micro-sized chromium(III) particles on cytotoxicity and gene expression profiles related to genomic stability in human keratinocytes and alveolar epithelial cells. *Nanomaterials*, *12*, 1294. https://doi.org/10.3390/nano12081294

[32] Zhao, J., Yu, L., Ma, H., Zhou, F., Yang, K., & Wu, G. (2020). Corn stalk-based activated carbon synthesized by a novel activation method for high-performance adsorption of hexavalent chromium in aqueous solutions. *Journal of Colloid and Interface Science*, *578*, 650-659. https://doi.org/10.1016/j.jcis.2020.06.031

[33] Tran, H. N., You, S.-J., Hosseini-Bandegharaei, A., & Chao, H.-P. (2017). Mistakes and inconsistencies regarding adsorption of contaminants from aqueous solutions: A critical review. *Water Research*, *120*, 88-116. https://doi.org/10.1016/j.watres.2017.04.014

[34] Tran, H. N., Lima, E. C., Juang, R.-S., Bollinger, J.-C., & Chao, H.-P. (2021). Thermodynamic parameters of liquid–phase adsorption process calculated from different equilibrium constants related to adsorption isotherms: A comparison study. *Journal of Environmental Chemical Engineering*, 9(6), 106674. https://doi.org/10.1016/j.jece.2021.106674

[35] Tran, H. N., Chao, H.-P., & You, S.-J. (2018). Activated carbons from golden shower upon different chemical activation methods: Synthesis and characterizations. *Adsorption Science & Technology*, *36*, 95-113. https://doi.org/10.1177/0263617416684837

[36] Pakade, V. E., Madikizela, L. M., Klink, M. J., & Ncube, S. (2023). Adsorption of toxic heavy metals using charred and uncharred coffee waste adsorbents: A review. *Environmental Technology Reviews*, *12*, 359-389. https://doi.org/10.1080/21622515.2023.2215459

[37] Kirishnamaline, G., Magdaline, J. D., Chithambarathanu, T., Aruldhas, D., & Anuf, A. R. (2021). Theoretical investigation of structure, anticancer activity and molecular docking of thiourea derivatives. *Journal of Molecular Structure*, *1225*, 129118. https://doi.org/10.1016/j.molstruc.2020.129118

[38] Vu, N.-T., & Do, K.-U. (2023). Insights into adsorption of ammonium by biochar derived from low temperature pyrolysis of coffee husk. *Biomass Conversion and Biorefinery*, *13*, 2193-2205. https://doi.org/10.1007/s13399-021-01337-9

[39] Liu, X., Renard, C. M., Bureau, S., & Le Bourvellec, C. (2021). Revisiting the contribution of ATR-FTIR spectroscopy to characterize plant cell wall polysaccharides. *Carbohydrate Polymers*, *262*, 117935. https://doi.org/10.1016/j.carbpol.2021.117935

[40] Zhao, N., Zhao, C., Tsang, D. C., Liu, K., Zhu, L., Zhang, W., Zhang, J., Tang, Y., & Qiu, R. (2021). Microscopic mechanism about the selective adsorption of Cr(VI) from salt solution on O-rich and N-rich biochars. *Journal of Hazardous Materials*, *404*, 124162. https://doi.org/10.1016/j.jhazmat.2020.124162

[41] Liu, C., Jin, R.-N., Ouyang, X.-k., & Wang, Y.-G. (2017). Adsorption behavior of carboxylated cellulose nanocrystal—polyethyleneimine composite for removal of Cr(VI) ions. *Applied Surface Science*, *408*, 77-87. https://doi.org/10.1016/j.apsusc.2017.02.265

[42] Long, X. l., Chen, P. y., & Jin, X. y. (2024). Effect of modification with hydrobromic acid on the performance of activated carbon in the removal of hexavalent chromium from aqueous solution. *Environmental Progress & Sustainable Energy*, *43*, e14245. https://doi.org/10.1002/ep.14245

[43] Chen, M., He, F., Hu, D., Bao, C., & Huang, Q. (2020). Broadened operating pH range for adsorption/reduction of aqueous Cr(VI) using biochar from directly treated jute (Corchorus capsularis L.) fibers by H3PO4. *Chemical Engineering Journal*, *381*, 122739. https://doi.org/10.1016/j.cej.2019.122739

[44] Tran, H. N., Nguyen, D. T., Le, G. T., Tomul, F., Lima, E. C., Woo, S. H., Sarmah, A. K., Nguyen, H. Q., Nguyen, P. T., & Nguyen, D. D. (2019). Adsorption mechanism of hexavalent chromium onto layered double hydroxides-based adsorbents: A systematic in-depth review. *Journal of Hazardous Materials*, *373*, 258-270. https://doi.org/10.1016/j.jhazmat.2019.03.018

[45] Gholipour, M., Hashemipour, H., & Mollashahi, M. (2011). Hexavalent chromium removal from aqueous solution via adsorption on granular activated carbon: Adsorption, desorption, modeling and simulation studies. *Journal of Engineering and Applied Sciences*, *6*, 10-18.

[46] Lin, C., Luo, W., Luo, T., Zhou, Q., Li, H., & Jing, L. (2018). A study on adsorption of Cr(VI) by modified rice straw: Characteristics, performances and mechanism. *Journal of Cleaner Production*, *196*, 626-634. https://doi.org/10.1016/j.jclepro.2018.05.279

[47] Wu, J., Yan, X., Li, L., Gu, J., Zhang, T., Tian, L., Su, X., & Lin, Z. (2021). High-efficiency adsorption of Cr(VI) and RhB by hierarchical porous carbon prepared from coal gangue. *Chemosphere*, *275*, 130008. https://doi.org/10.1016/j.chemosphere.2021.130008

[48] Zhou, H., & Chen, Y. (2010). Effect of acidic surface functional groups on Cr(VI) removal by activated carbon from aqueous solution. *Rare Metals*, *29*, 333-338. https://doi.org/10.1007/s12598-010-0059-6

[49] Demiral, H., Demiral, I., Tümsek, F., & Karabacakoğlu, B. (2008). Adsorption of chromium(VI) from aqueous solution by activated carbon derived from olive bagasse

and applicability of different adsorption models. *Chemical Engineering Journal*, *144*, 188-196. https://doi.org/10.1016/j.cej.2008.01.020

[50] Zhang, X., Zhang, L., & Li, A. (2018). Eucalyptus sawdust derived biochar generated by combining the hydrothermal carbonization and low concentration KOH modification for hexavalent chromium removal. *Journal of Environmental Management*, *206*, 989-998. https://doi.org/10.1016/j.jenvman.2017.11.079

[51] Labied, R., Benturki, O., Eddine Hamitouche, A. Y., & Donnot, A. (2018). Adsorption of hexavalent chromium by activated carbon obtained from a waste lignocellulosic material (Ziziphus jujuba cores): Kinetic, equilibrium, and thermodynamic study. *Adsorption Science & Technology*, *36*, 1066-1099. https://doi.org/10.1177/0263617417750739

[52] Lima, É. C., Adebayo, M. A., & Machado, F. M. (2015). Kinetic and equilibrium models of adsorption. In *Carbon nanomaterials as adsorbents for environmental and biological applications* (pp. 33-69). Springer.

[53] Wang, J., & Guo, X. (2020). Adsorption isotherm models: Classification, physical meaning, application and solving method. *Chemosphere*, *258*, 127279. https://doi.org/10.1016/j.chemosphere.2020.127279

[54] Cao, Y., Dong, S., Dai, Z., Zhu, L., Xiao, T., Zhang, X., Yin, S., & Soltanian, M. R. (2021). Adsorption model identification for chromium(VI) transport in unconsolidated sediments. *Journal of Hydrology*, *598*, 126228. https://doi.org/10.1016/j.jhydrol.2021.126228

[55] Jiang, F., Wei, C., Yu, Z., Ji, L., Liu, M., Cao, Q., Wu, L., & Li, F. (2023). Fabrication of iron-containing biochar by one-step ball milling for Cr(VI) and tetracycline removal from wastewater. *Langmuir*, *39*, 18958-18970. https://doi.org/10.1021/acs.langmuir.3c02885

[56] Wu, Z., Zhang, H., Ali, E., Shahab, A., Huang, H., Ullah, H., & Zeng, H. (2023). Synthesis of novel magnetic activated carbon for effective Cr(VI) removal via synergistic adsorption and chemical reduction. *Environmental Technology & Innovation*, *30*, 103092. https://doi.org/10.1016/j.envres.2022.114616

[57] Liu, L., Cai, W., Dang, C., Han, B., Chen, Y., Yi, R., Fan, J., Zhou, J., & Wei, J. (2020). One-step vapor-phase assisted hydrothermal synthesis of functionalized carbons: Effects of surface groups on their physicochemical properties and adsorption performance for Cr(VI). *Applied Surface Science*, *528*, 146984. https://doi.org/10.1016/j.apsusc.2020.146984

[58] Khosravi, R., Moussavi, G., Ghaneian, M. T., Ehrampoush, M. H., Barikbin, B., Ebrahimi, A. A., & Sharifzadeh, G. (2018). Chromium adsorption from aqueous solution using novel green nanocomposite: Adsorbent characterization, isotherm, kinetic and thermodynamic investigation. *Journal of Molecular Liquids*, *256*, 163-174. https://doi.org/10.1016/j.molliq.2018.02.033

[59] Sodkouieh, S. M., Kalantari, M., & Shamspur, T. (2023). Methylene blue adsorption by wheat straw-based adsorbents: Study of adsorption kinetics and isotherms. *Korean Journal of Chemical Engineering*, *40*, 873-881. https://doi.org/10.1007/s11814-022-1230-0

[60] Akram, M., Bhatti, H. N., Iqbal, M., Noreen, S., & Sadaf, S. (2017). Biocomposite efficiency for Cr(VI) adsorption: Kinetic, equilibrium and thermodynamics studies. *Journal of Environmental Chemical Engineering*, *5*, 400-411. https://doi.org/10.1016/j.jece.2016.12.002

[61] Islam, M. A., Angove, M. J., & Morton, D. W. (2019). Recent innovative research on chromium(VI) adsorption mechanism. *Environmental Nanotechnology, Monitoring & Management*, *12*, 100267. https://doi.org/10.1016/j.enmm.2019.100267

[62] Liu, W., Zhang, J., Zhang, C., Wang, Y., & Li, Y. (2010). Adsorptive removal of Cr(VI) by Fe-modified activated carbon prepared from Trapa natans husk. *Chemical Engineering Journal*, *162*, 677-684. https://doi.org/10.1016/j.cej.2010.06.020

[63] Luo, T., Xing, X., Zhang, X., Yue, W., & Ma, X. (2023). Efficient adsorption on Cr(VI) and electrochemical application of N, P co-doped carbon spheres. *Korean Journal of Chemical Engineering*, *40*, 2826-2838. https://doi.org/10.1007/s11814-023-1514-z

[64] Pamidimukkala, P. S., & Soni, H. (2018). Efficient removal of organic pollutants with activated carbon derived from palm shell: Spectroscopic characterization and experimental optimization. *Journal of Environmental Chemical Engineering*, *6*, 3135-3149. https://doi.org/10.1016/j.jece.2018.04.013

[65] Chen, Q., & Wu, Q. (2015). Preparation of carbon microspheres decorated with silver nanoparticles and their ability to remove dyes from aqueous solution. *Journal of Hazardous Materials*, *283*, 193-201. https://doi.org/10.1016/j.jhazmat.2014.09.024

[66] Nguyen, V.-T., Dat, N. D., Do, Q.-H., Le, V.-A., Truong, Q.-M., Nguyen, T.-B., Tran, A. T. K., Nguyen, M. L., Hoang, N. T.-T., & My, T. T. A. (2024). Modified sucrose biochar goethite (α-FeOOH): A potential adsorbent for methylene blue removal. *Korean Journal of Chemical Engineering*, 1-12. https://doi.org/10.1007/s11814-024-00237-8

[67] González-López, M. E., Laureano-Anzaldo, C. M., Pérez-Fonseca, A. A., Arellano, M., & Robledo-Ortíz, J. R. (2021). Chemically modified polysaccharides for hexavalent chromium adsorption. *Separation and Purification Reviews*, *50*, 333-362. https://doi.org/10.1080/15422119.2020.1783311

[68] Babapour, M., Dehghani, M. H., Alimohammadi, M., Arjmand, M. M., Salari, M., Rasuli, L., Mubarak, N. M., & Khan, N. A. (2022). Adsorption of Cr(VI) from aqueous solution using mesoporous metal-organic framework-5 functionalized with the amino acids: Characterization, optimization, linear and nonlinear kinetic models. *Journal of Molecular Liquids*, *345*, 117835. https://doi.org/10.1016/j.molliq.2021.117835

[69] Daneshvar, E., Zarrinmehr, M. J., Kousha, M., Hashtjin, A. M., Saratale, G. D., Maiti, A., Vithanage, M., & Bhatnagar, A. (2019). Hexavalent chromium removal from water by microalgal-based materials: Adsorption, desorption and recovery studies. *Bioresource Technology*, *293*, 122064. https://doi.org/10.1016/j.biortech.2019.122064

[70] Santhosh, C., Daneshvar, E., Tripathi, K. M., Baltrėnas, P., Kim, T., Baltrėnaitė, E., & Bhatnagar, A. (2020). Synthesis and characterization of magnetic biochar adsorbents for the removal of Cr(VI) and acid orange 7 dye from aqueous solution. *Environmental Science and Pollution Research International*, *27*, 32874-32887. https://doi.org/10.1007/s11356-020-09275-1

[71] Sun, Z., Liu, B., Li, M., Li, C., & Zheng, S. (2020). Carboxyl-rich carbon nanocomposite based on natural diatomite as adsorbent for efficient removal of Cr(VI). *Journal of Materials Research and Technology*, *9*, 948-959. https://doi.org/10.1016/j.jmrt.2019.11.034

[72] Zhang, B., Zhu, Z., Wang, X., Liu, X., & Kapteijn, F. (2024). Water adsorption in MOFs: Structures and applications. *Advanced Functional Materials*, *34*, 2304788. https://doi.org/10.1002/adfm.202304788

[73] Castro-Castro, J. D., Macías-Quiroga, I. F., Giraldo-Gómez, G. I., & Sanabria-González, N. R. (2020). Adsorption of Cr(VI) in aqueous solution using a surfactant-modified bentonite. *The Scientific World Journal*, *2020*, 3628163. https://doi.org/10.1155/2020/3628163

[74] Gan, C., Liu, Y., Tan, X., Wang, S., Zeng, G., Zheng, B., Li, T., Jiang, Z., & Liu, W. (2015). Effect of porous zinc–biochar nanocomposites on Cr(VI) adsorption from aqueous solution. *RSC Advances*, *5*, 35107-35115. https://doi.org/10.1039/C5RA04416B

[75] Zimmermann, A. C., Mecabô, A., Fagundes, T., & Rodrigues, C. A. (2010). Adsorption of Cr(VI) using Fe-crosslinked chitosan complex (Ch-Fe). *Journal of Hazardous Materials*, *179*, 192-196. https://doi.org/10.1016/j.jhazmat.2010.02.078

[76] Rajapaksha, A. U., Selvasembian, R., Ashiq, A., Gunarathne, V., Ekanayake, A., Perera, V., Wijesekera, H., Mia, S., Ahmad, M., & Vithanage, M. (2022). A systematic review on adsorptive removal of hexavalent chromium from aqueous solutions: Recent advances. *Science of the Total Environment*, *809*, 152055. https://doi.org/10.1016/j.scitotenv.2021.152055

[77] Elangovan, R., Philip, L., & Chandraraj, K. (2008). Biosorption of chromium species by aquatic weeds: Kinetics and mechanism

studies. *Journal of Hazardous Materials*, *152*, 100-112. https://doi.org/10.1016/j.jhazmat.2007.06.067

[78] Miretzky, P., & Cirelli, A. F. (2010). Cr(VI) and Cr(III) removal from aqueous solution by raw and modified lignocellulosic materials: A review. *Journal of Hazardous Materials*, *180*, 1-19. https://doi.org/10.1016/j.jhazmat.2010.04.060

How to cite this paper:

Dat, N. D., Huynh, S. Q., Nguyen, L. M. & Tran, H. N. (2026). Adsorption of hexavalent chromium from aqueous solution using glucose-derived spherical activated carbon: The role of functional groups. Advances in Environmental Technology, 12(3), 308-326. DOI: 10.22104/aet.2026.7860.2207